

# Future ramifications of age-dependent immunity levels for measles: explorations in an individual-based model

Elise Kuylen<sup>1,2</sup>, Lander Willem<sup>2</sup>, Niel Hens<sup>2,3</sup>, and Jan Broeckhove<sup>1</sup>

<sup>1</sup> IDLab, Department of Mathematics and Computer Science, University of Antwerp, Antwerp, Belgium

<sup>2</sup> CHERMID, Vaccine and Infectious Disease Institute, University of Antwerp, Antwerp, Belgium

<sup>3</sup> Interuniversity Institute for Biostatistics and statistical Bioinformatics, UHasselt, Hasselt, Belgium.

**Abstract.** When a high population immunity already exists for a disease, heterogeneities, such as social contact behavior and preventive behavior, become more important to understand the spread of this disease. Individual-based models are suited to investigate the effects of these heterogeneities. Measles is a disease for which, in many regions, high population immunity exists. However, different levels of immunity are observed for different age groups. For example, the generation born between 1985 and 1995 in Flanders is incompletely vaccinated, and thus has a higher level of susceptibility. As time progresses, this peak in susceptibility will shift to an older age category. Simultaneously, susceptibility will increase due to the waning of vaccine-induced immunity. Older generations, with a high degree of natural immunity, will, on the other hand, eventually disappear from the population. Using an individual-based model, we investigate the impact of changing age-dependent immunity levels (projected for Flanders, for years 2013 to 2040) on the risk for measles outbreaks. We find that, as time progresses, the risk for measles outbreaks increases, and outbreaks tend to be larger. As such, it is important to not only consider infants when designing strategies for measles elimination, but to also take other age categories into account.

**Keywords:** Individual-based modeling · Epidemiology · Measles · Immunity.

## 1 Introduction

Over the last decade, individual-based models have become increasingly popular within the domain of epidemiology [25]. In such a model, each individual is represented as a unique entity, thus offering the advantage of being able to model different levels of heterogeneity within a population. This makes it possible to incorporate system properties emerging from the unique behavior of several thousands or millions of individuals. Examples of heterogeneities that

may be of importance for epidemiological models are social contact behavior, susceptibility, and preventive behavior - such as vaccination. Heterogeneity is especially important in the case of emerging diseases and diseases for which a high population immunity already exists [3].

This is true for measles, a vaccine-preventable disease that - at the moment - mainly affects young children and still caused approximately 110 000 deaths worldwide in 2017 [26]. Understandably, an important goal that the WHO has set is the global eradication of measles. To reach this goal, the WHO proposes a target vaccination coverage with two doses of the vaccine of 95% of children in a country, to ensure the entire population is protected from outbreaks through herd immunity [27]. As such, focus is often placed on the immunization of infants and young children.

However, older age groups are often ignored when estimating the risk for measles outbreaks and planning for their prevention [11]. In Belgium, the vaccine against measles was included in the basic vaccination scheme in 1985 [5]. Individuals born before this date have often been infected with measles in the past. As it is assumed that individuals who survive a measles infection acquire lifelong immunity, this age group is expected to have a high level of immunity. This was confirmed by a recent serological survey conducted in Belgium [20].

However, the generation born between 1985 and 1995 is incompletely vaccinated as a result of the introduction period of the vaccine [5]. In the future, their immunity level is expected to decrease, due to waning of vaccine-induced immunity. Recent multi-country surveys confirm that a growing fraction of susceptibles to measles are adolescents and young adults, indicating the need to focus on these age groups when planning for measles elimination [2, 21, 22]. This is also the conclusion of a study which aimed to determine age-dependent susceptibility to measles in Japan [14]. They conclude that supplementary vaccination for adults between 20 and 49 years old would be useful to prevent future outbreaks of measles.

The decades after the vaccine was introduced, uptake steadily increased - thus lowering the number of individuals susceptible to measles. This, in turn, led to a decrease in measles infections. Because of this, in combination with the aging of the generation born before the introduction of the vaccine, natural immunity has become less frequent. As of 2016, 96.2% of infants in Flanders, Belgium are vaccinated with the first dose of the MMR vaccine [4]. However, due to false reports on side-effects of the MMR (Measles - Mumps - Rubella) vaccine, vaccination levels have recently been declining in several countries - putting them at risk for dropping below the 95% immunization target [13].

The combination of these factors makes it necessary to look at the impact of different vaccination levels for different age groups on the risk of measles outbreaks, today as well as in the future. This is highlighted by a new analysis, which takes into account age-dependent social contact patterns to estimate herd immunity thresholds for different age categories [10].

A recent study [12] investigated how immunity levels for different age groups in Flanders could change in the future. They predict that, as a result of the

factors described above, not only will age-dependent immunity levels shift in the future, but overall susceptibility to measles will also be higher. An individual-based model is particularly suited to investigate the impact of changing immunity levels in the future, because it is possible to model person-to-person interactions that differ based on age and on context of the interaction (e.g. schools, workplaces, daycare centers).

In this paper, we extend the individual-based model Stride [15] to include age-dependent immunity levels. We investigate the impact on outbreak occurrence and outbreak size of the shifting age-dependent immunity levels in Flanders for 6 different years from 2013 to 2040. We show that, as time progresses, the risk for a measles outbreak in Flanders increases, as does the predicted size of such an outbreak. Furthermore, in addition to infants, other age-groups experience a growing risk for measles infection.

## 2 Methods

We used Stride, an individual-based simulator for the transmission of infectious diseases [15]. Stride is a stochastic model: processes such as contacts between individuals and disease transmission have a probabilistic component. Furthermore, Stride is designed to be very versatile. By using different input files, it is possible to run simulations for a multitude of populations and diseases. The core logic of Stride is implemented in C++, making it highly portable and open to performance-optimization [23]. Finally, Stride is developed as an open-source project: its code can be found in a public Github repository [6]. More information about the structure and internal logic of Stride can be found in a previous publication [15].

We modified Stride to implement age-dependent immunity levels. Before the beginning of the actual simulation, the population is set up. During this process, each individual in the population is marked either susceptible or immune to the simulated disease. We use a target fraction of immune individuals for each age between 0 and 99 years. The unit of the age categories is one year. For each age category, we first calculate the target number of immune individuals, based on the immunity level and the total number of individuals in the age category. Next, we check for each randomly drawn person, whether the age bracket to which they belong contains enough immune individuals. If it does not, we mark the selected individual ‘immune’ and continue to randomly draw another individual from the population. We continue this process until all age brackets contain the target number of immune individuals.

We ran simulations for 6 different years from 2013 to 2040 (2013, 2020, 2025, 2030, 2035, 2040). The age-dependent immunity levels for each year that we used, were based on results from [12], and were obtained through personal communication with the authors. We received projections of immunity levels for the years mentioned above, for 500 municipalities in Belgium. To obtain the immunity levels that we used for our simulations, we took the average fraction of immune individuals for each age category over 500 bootstrap runs for all mu-

municipalities. All municipalities were treated the same: size differences between municipalities were not taken into account in calculating the mean immunity level per age category.

For comparison, we also ran simulations for each of the six calendar years using a constant immunity level which was identical over all age categories. The immunity levels used for these simulations were based on averages obtained from previous simulations that used age-dependent immunity levels. An overview of the average immunity level per simulated calendar year can be found in Table 1.

Immunity data for ages 0 to 85 years was available. Since Stride includes individuals up to 99 years of age, immunity levels for ages between 86 and 99 years were assumed to be the same as the immunity level for 85 year olds. Age-dependent susceptibility levels (1 - fraction of immune individuals in age category) that were used for each examined year can be seen in Figure 1 (left).

The population we use consists of 600 000 individuals, representing a sample of the total population of Flanders - which consists of about 6 million people. The synthetic population is made up out of reference households, obtained from a survey in 2010–2011 [24]. Geographic distribution of these households is based on 2001 census data. Children are assigned to a daycare (0–2 years old), preschool (3–5 years old), primary (6–11 years old), secondary (12–17 years old) or tertiary (18–23 years old) school based on enrollment statistics acquired from Eurostat [8]. Adults (18–64 years old) are assigned to a workplace based on age-specific employment data and aggregated workplace size data from Eurostat and commuting data from the 2001 census. To account for general contacts, all individuals are also assigned to two ‘communities’. One of these represents the general contacts made during the week, while the other represents those made during the weekend. We distinguish these two types of community for two reasons. Firstly, different contact rates apply for weekdays and weekend days. Secondly, by letting individuals make general contacts within two different communities, we are able to model the movement of an infectious disease between communities. Each community consists of 1000 individuals on average, which is in line with the size of communities used in a previous model [7].

The population is closed, meaning that no individuals are born or die over the course of the simulation. The contact rates that determine the probability of a contact occurring between two individuals of certain ages at a given location are based on data from a social contact survey in Flanders [24]. Separate social contact patterns are used for weekdays and weekend days. Holidays - both school and regular - are not taken into account.

We ran each simulation for 730 time-steps, which corresponds to 2 simulated years. This was done to allow each epidemic to run its course, until no more new infections were being recorded. At the beginning of each simulation, a single individual in the population is selected, and their health status is set to ‘infected’. The natural history of the disease was modeled as follows. At the beginning of a simulation, it is determined for each individual how long it takes until they become infectious after becoming infected, how long it takes until they become symptomatic and finally, how long it takes for them to recover. Each

of these durations is drawn from a distribution. Incubation periods are sampled from a lognormal distribution with median 12.5 and dispersion 1.25 [16]. After this period, individuals become infectious, which lasts 6 to 8 days [1]. After either 2 or 3 days of being infectious but asymptomatic, individuals begin to experience symptoms of their disease. This symptomatic period, during which persons stay at home and thus only make contacts within their household, lasts 6 to 8 days. In our model, we assume that each infected individual eventually becomes symptomatic.

When an infected individual has a contact with a susceptible individual, a chance for disease transmission exists. The probability for such a transmission event is calculated from the basic reproduction number  $R_0$ , which is supplied as an input parameter. For each calendar year that we simulated between 2013 and 2040, we tested input values of  $R_0$  between 12 and 18, as the basic reproduction number for measles is commonly estimated to be in this range [9].

The relation between  $R_0$  and the transmission probability was estimated by fitting a function to data resulting from a large number of simulations [7]. We tested 21 values for the transmission probability between 0 and 1, and started simulations on 7 different days of the week, to account for different contact rates during weekdays and weekend days. To obtain stable results, we ran 150 stochastic simulations for each of these scenarios, resulting in a total of 22050 runs.

At the beginning of each simulation, one infected individual was introduced into the population. All other individuals in the population were initialized as susceptible. Other parameters were identical to those used in the experiments described in this paper.

During each simulation, we tracked the number of secondary cases one infected individual caused in the completely susceptible population. We fitted the data-points we obtained to a quadratic function using the ‘polyfit’ method from the numpy Python package [17]. As such we derived the formula in Equation (1).

$$\hat{R}_0 = 0 + 32.862 * P(\text{transmission}) - 6.184 * P(\text{transmission})^2 \quad (1)$$

Before the beginning of the simulation, after the population has been set up, we record for each individual their age in years and whether or not they are susceptible to the simulated disease. During each time-step of the simulation - which corresponds to one day - we keep track of how many individuals have been infected until then. This also includes individuals who have since recovered from the disease.

We executed 200 stochastic simulation for each combination of calendar year and  $R_0$ . Seeds to initiate our random number generator were generated from a non-deterministic, machine-specific source. To improve performance, several simulations were run in parallel, using the Python environment we created for Stride and the Python ‘multiprocessing’ package [19]. All simulations were run on a Linux machine, using 8 cores (16 threads).

### 3 Results

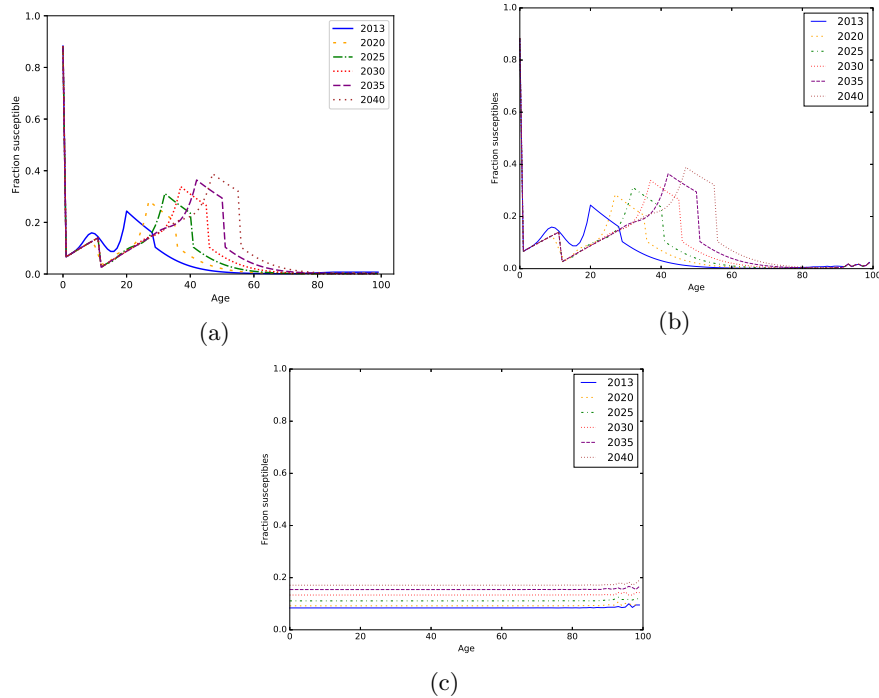


**Fig. 1.** Upper left (a): the projected fraction of susceptibles by age (in years) for years 2013–2040. Projections were based on a previous study [12]. Upper right (b): age-dependent susceptibility levels as observed in simulated populations for years 2013–2040, when using age-dependent immunity levels based on (a). Lower row, middle (c): age-dependent susceptibility levels as observed in simulated populations for years 2013–2040, when using uniform immunity levels for all age categories.

From the information on each individual’s susceptibility, recorded at the beginning of every simulation, we calculated average age-dependent susceptibility levels. These are displayed in Figure 1 (b), and are very close to the projected levels for each year, which are shown in Figure 1 (a). We observe that in 2013, there is a peak in susceptibility for individuals between - roughly - 18 and 28 years old, the generation born between 1985 and 1995. As time progresses, this peak shifts to an older age group. It also increases in height, as a result of the waning of vaccine-induced immunity. Vaccination coverage for infants and children remains stable.

We did the same for the simulations using uniform immunity levels for all age categories, the results of which can be seen in Figure 1 (c). The uniform

immunity levels that were used for calendar years 2013–2040 can be found in Table 1. We see that, due to the number of individuals having natural immunity decreasing and the waning of vaccine-induced immunity, the overall immunity lowers as time progresses. Small variations in the oldest age categories can be attributed to a limited number of individuals of these ages being present in the simulated population.

**Table 1.** Percentage of immune individuals in the population for simulated years 2013, 2020, 2025, 2030, 2035 and 2040.

Year	Percentage immune
2013	91.61 %
2020	90.81 %
2025	88.91 %
2030	86.67 %
2035	84.57 %
2040	82.90 %

To get an idea of how often the introduction of an infected individual in the population leads to an actual outbreak, we first estimated an ‘extinction threshold’. To do this, a histogram of the total number of infections at the end of each simulation was created. In Figure 2, an overview of the results for the simulations with age-dependent immunity levels and  $R_0$  12 can be seen. We created the same histogram for simulations that used a uniform immunity level for all age categories, and for simulations with  $R_0$  values of 13, 14, 15, 16, 17 and 18. These yielded similar results, which are not shown here.

For each simulated calendar year, there is a certain fraction of runs where the epidemic dies out without causing many - or even any - secondary infections. We will refer to these as the extinction cases. To get a realistic idea of the size and frequency of outbreaks when no such extinction occurs, we set an ‘extinction threshold’. When the total number of infected cases at the end of a simulation was higher than this threshold, we say that an outbreak occurred. Otherwise, the run was regarded as an extinction case. Using the results shown in Figure 2 and similar histograms for other scenarios, we set the extinction threshold at 10 000 cases. A clear division can be seen: either the number of infected cases is close to zero, or there are at least 10 000 cases.

Using this threshold, we calculated the fraction of simulation runs for each combination of simulated year and  $R_0$  value that resulted in an outbreak, both for simulations using age-dependent immunity levels and for simulations using uniform levels for all age categories. These results can be observed in Figure 3. We can see that the fraction of outbreak occurrences increases as time progresses. This is the case when using age-dependent immunity levels as well as for simulations using uniform immunity levels. However, we can see that when age-dependent immunity levels are taken into account (Figure 3 (a)) the fraction of runs that leads to an outbreak is higher in the first simulated calendar

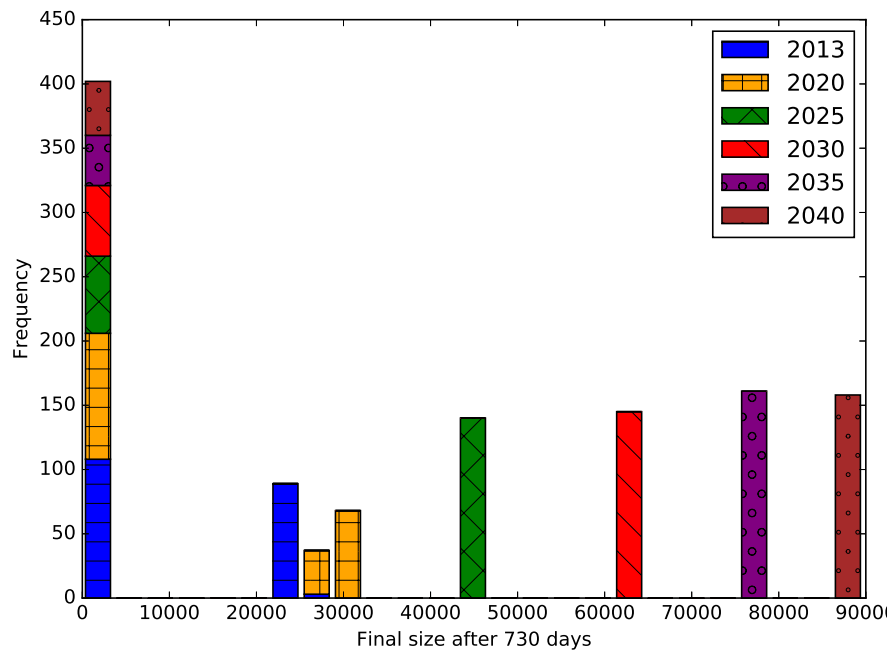


**Fig. 2.** Outbreak size frequencies, plotted by simulated calendar year (shown here for  $R_0$  12 and for simulations using age-dependent immunity levels). For each simulated year shown here, 200 stochastic simulations were run.



years compared to simulations using uniform immunity levels (Figure 3 (b)). We included results for simulations with values for  $R_0$  of 12 (blue circles) and 18 (green triangles) (results for  $R_0$  12, 14, 15, 16 and 17 not shown). The increasing trend can be observed for both  $R_0$  values shown, but is less pronounced for higher values of  $R_0$ .

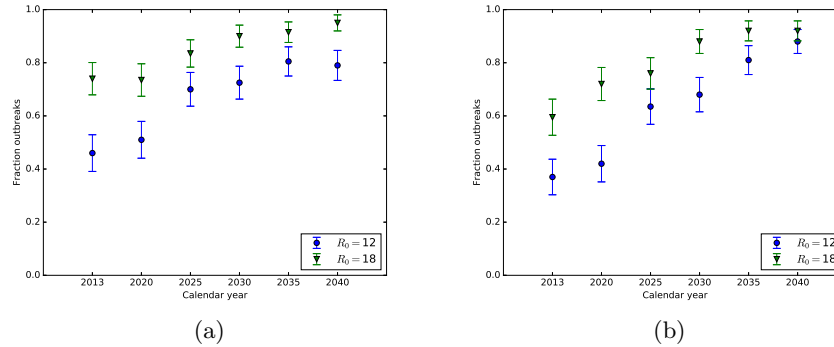


**Fig. 3.** Comparison of the fraction of simulation runs (out of 200) that result in an outbreak (extinction threshold = 10 000 cases) for simulations using age-dependent immunity levels (a) and uniform immunity levels for all age categories (b). Results shown here for  $R_0$  12 and 18. Error bars indicate 95% percentile intervals.

We also consider the final size of outbreaks when no extinction occurred. In Figure 4, the distribution of outbreak sizes can be seen for simulations using age-dependent immunity levels (a) and uniform immunity levels for all age categories (b). In both cases, outbreak sizes increase as time progresses. However, when taking age-dependent immunity levels into account (a), the increase in size is slower in earlier years, and has a sharp increase from 2025 onward. On the other hand, for simulations using uniform immunity levels for all age categories (b), the increase in outbreak sizes is more linear. Furthermore, outbreak sizes in 2013 are already higher in the first case (a), compared to simulations in which immunity levels are uniform for all age categories (b). However, as time progresses the difference between (a) and (b) becomes less pronounced.

Results for  $R_0$  values of both 12 and 18 can be observed in Figure 4. The same general trends can be observed for runs with  $R_0$  values of 13, 14, 15, 16 and 17, for which the results are not shown here.

We ran a total of 16800 simulations: 200 runs for 7 values of  $R_0$  (12, 13, 14, 15, 16, 17 and 18) and 6 different simulated years (2013, 2020, 2025, 2030, 2035 and 2040), both using age-dependent immunity levels and uniform immunity levels for all age categories. It took about 26 hours to run these, using 16 workers in the Python multiprocessing pool.

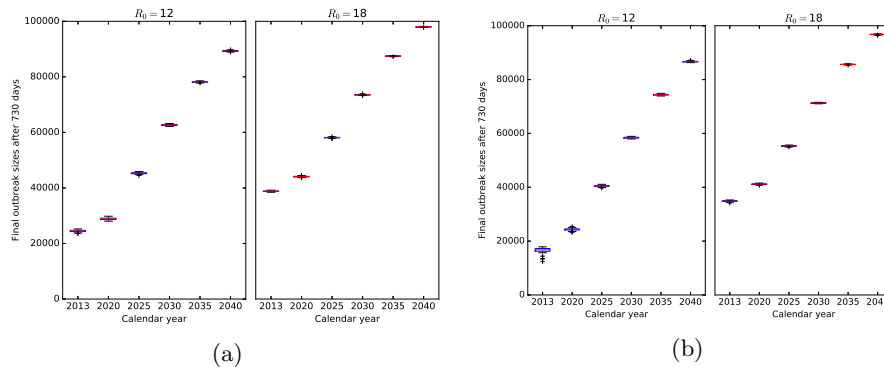


**Fig. 4.** Comparison of final outbreak sizes for simulations using age-dependent immunity levels (a) and uniform immunity levels for all age categories (b), when no extinction occurs (extinction threshold = 10 000 cases. Results here are shown for  $R_0$  values 12 and 18.

## 4 Discussion

We used an individual-based model to assess the impact of changing age-dependent immunity levels on the risk for measles outbreaks in Flanders. We were able to use detailed projections on the immunity levels of all ages from 0 to 85 years for calendar years 2013 to 2040. Since we used an individual-based model, we were also able to model contact rates that differed based on age and context. By doing this, instead of assuming homogeneous mixing, we could assess the impact of immunity levels differing by age more accurately.

We observed a difference between simulations that took into account age-dependent immunity levels and simulations where a uniform immunity level was assumed for all age categories. Even though average immunity levels were identical between these two scenarios for calendar years 2013 to 2040, we saw that when we took into account age-dependent immunity levels, the predicted risk for measles outbreaks was higher. This effect was the strongest in earlier calendar years, and became less pronounced as time progressed. When assuming uniform immunity levels for all age categories and an  $R_0$  value of 12 the probability of an outbreak occurring in 2020 is about 0.3. By contrast, when taking into account age-dependent immunity levels, this probability increases to about 0.5. For higher values of  $R_0$ , the same trend can be observed, but the effect is less strong. This confirms that heterogeneities in the population become more important for estimating the risk for a measles outbreak as the overall immunity level of the population increases or the value of  $R_0$  decreases. As we near the target of measles elimination, these will thus become more important when modeling the spread of this disease.

Furthermore, when outbreaks do occur, they are expected to become larger. This is because a larger part of the population will become susceptible to measles over time. The difference between the case in which age-dependent immunity

levels are taken into account and when uniform immunity levels are assumed is observable in earlier calendar years, but fades as time progresses. This suggests that larger outbreak sizes are mainly due to a larger number of susceptibles available in the population. The older generation, which still has natural immunity, ages and dies out, while the fraction of infants and children immunized remains stable. The immunity level of the generation born between 1985 and 1995 was already lower, and is expected to further decrease due to the waning of vaccine-induced immunity. As such, even though the vaccination coverage of infants and young children remains high, the overall susceptibility in the population increases.

Regarding these results, some limitations need to be considered. First, the population in Stride is closed. For childhood diseases such as measles, a model in which new infants can be born into the population could yield more accurate results. In future work, we wish to add a demographic component to Stride, that would make this possible.

Secondly, there were a few factors that were not yet considered in the projected age-dependent immunity rates that we used. As the projections were based on serological data collected in Belgium in 2006, only humoral immunity is taken into account [20]. However, recent studies [18] suggest that, in cases where there is no humoral immunity protecting an individual, they can still be protected against a disease through cellular immunity. As such, the projections made here would overestimate the susceptibility for measles in the population.

Furthermore, we note that, for the projections we used, the assumption is made that no large measles outbreaks occur until 2040, which would again increase natural immunity. Finally, in the projections that we used, the recent increase in vaccine hesitancy was not taken into account. Due to, among others, false reports on side-effects of the MMR vaccine, vaccine uptake has been decreasing in some countries [13]. This could cause an additional increase in susceptibility, besides the one that was discussed in this paper.

When taking into account age-dependent immunity levels, we observed that, while the immunity level for infants and young children remains stable, the risk for a measles outbreak increases as time progresses. Moreover, the size of such outbreaks is expected to increase. As such, it is important to consider age-dependent immunity levels when planning for the elimination of measles. Other age groups - besides infants and young children - should be given attention as well when designing vaccination strategies. To increase the vaccination coverage for individuals born between 1985 and 1995 a catch-up campaign could, for example, be organized.

Those born between 1985 and 1995 have reached the age of becoming parents themselves today. An opportunity would be to immunize those that were left unvaccinated as infants when they visit a doctor for the immunization of their own children. In future work, it could be interesting to investigate the cost-effectiveness of such a campaign.

Finally, it would also be interesting to conduct the same research for other vaccine-preventable diseases and other populations. Using Stride, this should be feasible when input data on population immunity levels is available.

## References

1. Anderson, R., May, R.: Infectious diseases of humans: dynamics and control. Oxford University Press (1992)
2. Andrews, N., Tischer, A., Siedler, A., Pebody, R., Barbara, C., Cotter, S., Duks, A., Gacheva, N., Bohumir, K., Johansen, K., Mossong, J., de Ory, F., Prosenec, K., Slcikov, M., Theeten, H., Zarvou, M., Pistol, A., Bartha, K., Cohen, D., Backhouse, J., Griskevicius, A., Nardonel, A.: Towards elimination: measles susceptibility in Australia and 17 European Countries. *Bulletin of the World Health Organisation* **86**, 197–204 (2008)
3. Béraud, G.: Mathematical models and vaccination strategies. *Vaccine* **36**(36), 5366–5372 (2018)
4. Braeckman, T., Theeten, H., Roelants, M., Blaizot, S., Hoppenbrouwers, K., Maertens, K., Van Damme, P., Vandermeulen, C.: Can Flanders resist the measles outbreak? Assessing vaccination coverage in different age groups among Flemish residents. *Epidemiology and Infection* **146**(8), 1043–1047 (2018)
5. Braeye, T., Sabbe, M., Hutse, V., Flipse, W., Godderis, L., Top, G.: Obstacles in measles elimination: an in-depth description of a measles outbreak in Ghent, Belgium, spring 2011. *Archives of Public Health* **71**(1), 17 (2013)
6. Broeckhove, J., Kuylen, E., Willem, L.: Stride Github repository. <https://github.com/broeckho/stride>
7. Chao, D., Halloran, M., Obenchain, V., Longini, I.: FluTE, a Publicly Available Stochastic Influenza Epidemic Simulation Model. *PLoS Comput Biol* **6**(1), e1000656 (2010)
8. European Commission: Eurostat. <https://ec.europa.eu/eurostat/>
9. Fine, P.: Herd immunity: history, theory, practice. *Epidemiologic reviews* **15**(2), 265–302 (1993)
10. Funk, S., Knapp, J., Lebo, E., Reef, S., Dabagh, A., Kretsinger, K., Jit, M., Edmunds, W., Strebel, P.: Target immunity levels for achieving and maintaining measles elimination. *BioRxiv* p. 201574 (2018)
11. Hayman, D.: Measles vaccination in an increasingly immunized and developed world. *Human Vaccines & Immunotherapeutics* (2018)
12. Hens, N., Abrams, S., Santermans, E., Theeten, H., Goeyvaerts, N., Lernout, T., Leuridan, E., Van Kerckhove, K., Goossens, H., Van Damme, P., Beutels, P.: Assessing the risk of measles resurgence in a highly vaccinated population: Belgium anno 2013. *Eurosurveillance* **20**(1), 20998 (2015)
13. Jansen, V., Stollenwerk, N., Jensen, H., Ramsay, M., Edmunds, W., Rhodes, C.: Measles Outbreaks in a Population with Declining Vaccine Uptake. *Science* **301**(5634), 804 (2003)
14. Kinoshita, R., Nishiura, H.: Assessing age-dependent susceptibility to measles in Japan. *Vaccine* **35**(25), 3309–3317 (2017)
15. Kuylen, E., Stijven, S., Broeckhove, J., Willem, L.: Social contact patterns in an individual-based simulator for the transmission of infectious diseases (Stride). *Procedia Computer Science* **108**, 2438–2442 (2017)

16. Lessler, J., Reich, N., Brookmeyer, R., Perl, T., Nelson, K., Cummings, D.: Incubation periods of acute respiratory viral infections: a systematic review. *Lancet Infect Dis* **9**, 291–300 (2009)
17. NumPy Developers: NumPy. <http://www.numpy.org/>, accessed: 2019-04-04
18. Plotkin, S.: Complex correlates of protection after vaccination. *Clinical infectious diseases* **56**(10), 1458–1465 (2013)
19. Python Software Foundation: Multiprocessing – Process-based parallelism. <https://docs.python.org/3.4/library/multiprocessing.html>, accessed: 2019-01-14
20. Theeten, H., Hutse, V., Hens, N., Yavuz, Y., Hoppenbrouwers, K., Beutels, P., Vranckx, R., Van Damme, P.: Are we hitting immunity targets? The 2006 age-specific seroprevalence of measles, mumps, rubella, diphtheria and tetanus in Belgium. *Epidemiology and Infection* **139**(4), 494–504 (2011)
21. Thompson, K.: What will it take to end human suffering from measles? *Lancet Infect Dis* **17**(10), 1013–1014 (2017)
22. Trentini, F., Poletti, P., Merler, S., Melegaro, A.: Measles immunity gaps and the progress towards elimination: a multi-country modelling analysis. *Lancet Infect Dis* **17**(10), 1089–1097 (2017)
23. Willem, L., Stijven, S., Tijskens, E., Beutels, P., Hens, N., Broeckhove, J.: Optimizing agent-based transmission models for infectious diseases. *BMC bioinformatics* **16**(1), 183 (2015)
24. Willem, L., Van Kerckhove, K., Chao, D., Hens, N., Beutels, P.: A nice day for an infection? Weather conditions and social contact patterns relevant to influenza transmission. *PLoS ONE* **7**(11), e48695 (2012)
25. Willem, L., Verelst, F., Bilcke, J., Hens, N., Beutels, P.: Lessons from a decade of individual-based models for infectious disease transmission: a systematic review (2006–2015). *BMC infectious diseases* **17**(1), 612 (2017)
26. World Health Organisation: Measles. <https://www.who.int/news-room/fact-sheets/detail/measles>, accessed: 2019-01-09
27. World Health Organisation: Measles vaccines: WHO position paper - April 2017. *Weekly epidemiological record* **92**(17), 205–228 (2017)